

Chemo-mechanical model for predicting the lifetime of epdm rubbers

Xavier Colin, Mouna Ben Hassine, Moussa Nait-Abelaziz

▶ **To cite this version:**

Xavier Colin, Mouna Ben Hassine, Moussa Nait-Abelaziz. Chemo-mechanical model for predicting the lifetime of epdm rubbers. Rubber Chemistry and Technology, 2019, 92 (4), pp.722-748. 10.5254/rct.19.81469 . hal-02734099

HAL Id: hal-02734099
https://hal.science/hal-02734099

Submitted on 2 Jun 2020

HAL is a multi-disciplinary open access archive for the deposit and dissemination of scientific research documents, whether they are published or not. The documents may come from teaching and research institutions in France or abroad, or from public or private research centers.

L'archive ouverte pluridisciplinaire **HAL**, est destinée au dépôt et à la diffusion de documents scientifiques de niveau recherche, publiés ou non, émanant des établissements d'enseignement et de recherche français ou étrangers, des laboratoires publics ou privés.

CHEMO-MECHANICAL MODEL FOR PREDICTING THE LIFETIME OF EPDM RUBBERS

XAVIER COLIN,[1,*] MOUNA BEN HASSINE,[2] MOUSSA NAIT-ABELAZIZ[3]

[1]LABORATORY PIMM, ARTS ET MÉTIERS PARISTECH, 75013 PARIS, FRANCE
[2]DEPARTMENT MMC, EDF LAB, 77818 MORET-SUR-LOING, FRANCE
[3]LML, UNIVERSITÉ DE LILLE 1, 59650 VILLENEUVE D'ASQ, FRANCE

ABSTRACT

A chemo-mechanical model has been developed for predicting the long-term mechanical behavior of EPDM rubbers in a harsh thermal oxidative environment. Schematically, this model is composed of two complementary levels: The "chemical level" calculates the degradation kinetics of the macromolecular network that is introduced into the "mechanical level" to deduce the corresponding mechanical behavior in tension. The "chemical level" is derived from a realistic mechanistic scheme composed of 19 elementary reactions describing the thermal oxidation of EPDM chains, their stabilization against oxidation by commercial antioxidants but also by sulfide bridges, and the maturation and reversion of the macromolecular network. The different rate constants and chemical yields have been determined from a heavy thermal aging campaign in air between 70 and 170 °C on four distinct EPDM formulations: additive free gum, unstabilized and stabilized sulfur vulcanized gum, and industrial material. This "chemical level" has been used as an inverse resolution method for simulating accurately the consequences of thermal aging at the molecular (concentration changes in antioxidants, carbonyl products, double bonds, and sulfide bridges), macromolecular (concentration changes in chain scissions and cross-link nodes), and macroscopic scales (weight changes). Finally, it gives access to the concentration changes in elastically active chains from which are deduced the corresponding changes in average molar mass M_C between two consecutive cross-link nodes. The "mechanical level" is derived from a modified version of the statistical theory of rubber elasticity, called the phantom network theory. It relates the elastic and fracture properties to M_C if considering the macromolecular network perfect, and gives access to the lifetime of the EPDM rubber based on a relevant structural or mechanical end-of-life criterion. A few examples of simulations are given to demonstrate the reliability of the chemo-mechanical model. [doi:10.5254/rct.19.81469]

INTRODUCTION

The thermal aging of elastomers has been the subject of much research work since the end of the 19th century. Research intensified in the early part of the 20th century, but the authors encountered insurmountable obstacles while two major concepts were not resolved: the concept of "free radical and chain reaction"[1] and the concept of "macromolecule."[2] The first one allowed the development of increasingly more consistent mechanistic and kinetic schemes. The second one allowed understanding chemical events responsible for the changes in mechanical properties, that is, chain scissions and cross-linking.

This discipline really took off at the end of the Second World War. At first, Rubber and Plastics Research Association (RAPRA) researchers[3,4] developed the "standard" mechanistic scheme for the oxidation of saturated hydrocarbon polymers, essentially justified by thermochemical considerations. Then, Tobolsky[5] derived a kinetic model from this mechanism. Unfortunately, the scientific community has ignored this model for a long time, despite its very high heuristic value.

After 1950, two axes of research were developed simultaneously. On one hand, chemists tried to provide a concrete basis to the "standard" mechanistic scheme by identifying the main oxidation products and checking the validity of their formation paths.[6–9] On the other hand, physicists analyzed the consequences of oxidation on mechanical behavior and tried to explain them by using the theory of polymer behavior in solution[10,11] or the statistical theory of rubber elasticity.[12] Today, one key question is still unsolved: How to connect these two axes of research? In other words:

Which elementary reactions of the "standard" mechanistic scheme are responsible for macromolecular changes? Chain scissions and/or cross-linking?

The period 1950–1990 was characterized by a proliferation of high-level scientific research. New key issues emerged, not only in terms of mechanisms, but also in terms of consequences of oxidation on mechanical behavior. Chemists highlighted all the complexities of oxidation reactions for unsaturated hydrocarbon polymers, for which propagation occurs as much by hydrogen abstraction, according to the "standard" mechanistic scheme,[3,4] as by addition of radical species onto double bonds.[6–9] However, the numerous attempts for relating the macromolecular changes to the mechanistic scheme led to results that were regarded as convincing, but also in many ways, contradictory.

During this period (1950–1990), the general rule was to look exclusively for analytical solutions in problems of chemical kinetics. However, these solutions were obtained by making a series of simplifying assumptions that are either restrictive or difficult to justify. Today, the commonly held view is that some of these assumptions lead to serious inaccuracies in model simulations and, consequently, to serious errors in interpretation of experimental results. This somewhat arbitrary approach is certainly one of the main reasons for the stagnation of this discipline in the 1980s. Fortunately, thanks to the progress in scientific and numerical computation, it is now possible to solve problems of chemical kinetics without resorting to simplifying assumptions, as well as solving oxidation problems involving a large number of elementary reactions, which were previously thought to be inextricable.[13,14]

The latest period, 2000–2019, is marked by the development of new analytical techniques[15–17] and theoretical tools[18,19] for better understanding and describing the structure of the macromolecular network, in particular in sulfur vulcanized rubbers. Thermoporosimetry[15,16] and double quantum nuclear magnetic resonance (DQ-NMR)[16,17] appear to be very sensitive and promising techniques for elucidating the relationships between the structure and mechanical properties of virgin and aged elastomers.

The aim of this work is to give an overview of the chemo-mechanical model developed for predicting the long-term mechanical behavior of EPDM rubbers and their lifetime in a harsh thermal oxidative environment for the French Electricity Agency (Électricité de France [EDF]). This multi-scale model is the result of a close collaboration between two complementary academic institutions: Laboratorie Procédés et Ingénierie en Mécanique et Matériaux (PIMM; specializing in kinetic analysis and modeling of aging mechanisms in polymers) and Laboratoire de Mécanique de Lille (LML; specializing in mechanical behavior of polymers). The latter organization is particularly adept at modeling the changes in mechanical behavior caused by external damage.

Essentially, the chemo-mechanical model comprises two simultaneous levels of analysis. The first level is chemical in nature (developed by PIMM), whereas the second one is purely mechanical (developed by LML). The "chemical level" calculates the degradation kinetics of the macromolecular network that is introduced into the "mechanical level" to deduce the corresponding mechanical behavior in tension. The "mechanical level" allows lifetime predictions to be made on polymers (EPDM rubber in the present case) after having decided upon a relevant structural or mechanical end-of-life criterion. We will present a few examples of simulations in this manuscript in order to demonstrate the reliability of the chemo-mechanical model.

THEORETICAL

CHEMICAL LEVEL

The "chemical level" is totally open. It is composed of a core common to all cases of thermal aging. This core is derived from the well-known "standard" mechanistic scheme.[3,4] It describes the thermal oxidation at low to moderate temperatures (typically for $T < 200\,^{\circ}\mathrm{C}$) and at low conversion

(2) $P^{\bullet} + O_2 \rightarrow PO_2^{\bullet}$ (k_2)
(3) $PO_2^{\bullet} + PH \rightarrow POOH + P^{\bullet}$ (k_3)

SCHEME 1. — Common propagation steps.

ratios of a saturated hydrocarbon polymer without any additives. In such a case, the main source of radicals is the thermal decomposition of the main propagation product: the hydroperoxide POOH.[20] This closed-loop character is effective in explaining the sharp auto-acceleration of oxidation at the end of the induction period. Around this core, as many layers as necessary are added to describe all the possible complexities of the problem to be solved.

Some layers take into account important elementary reactions initially neglected or overlooked in the "standard" mechanistic scheme. Other layers are devoted to the extension of this scheme to unsaturated hydrocarbon polymers. Some layers take into account the complexity of industrial formulations, in particular the stabilization by common blends of commercial antioxidants and reactive fillers such as carbon black. Other layers take into account the existence of non-radical chemical processes superposing on oxidation. In addition, other layers are devoted to the determination of molecular changes, but also of all other structural changes taking place at the macroscopic level and, therefore, responsible for the changes in mechanical properties. At the macromolecular scale, these changes are chain scissions and cross-linking. The last layer is dedicated to the calculation of the structural quantity allowing connection of the chemical and mechanical responses. When cross-linking predominates largely over chain scissions, which is the case in sulfur vulcanized elastomers,[21–24] the pertinent quantity of interest is the concentration of cross-link nodes or the average molar mass M_C between two consecutive cross-link nodes.

All layers discussed above are considered optional, that is, they are taken into account or neglected according to the complexity of the problem under consideration. However, the final "chemical level" is composed of the core and all layers, since it is easy for the user to set an initial concentration or a rate constant to zero to suppress the influence of any chosen layer.

Core of the "Chemical Level." — To date, all the mechanistic schemes proposed for accounting for the oxidation of hydrocarbon polymers are derived from the "standard" mechanistic scheme developed in the 1940s by the RAPRA researchers.[3,4] There is a general consensus on the fact that propagation is a two-step reaction (see Scheme 1). The first step is very fast and almost independent of temperature.[25] The corresponding rate constant k_2 is of the order of 10^8–10^9 L mol^{-1} s^{-1}. In contrast, the second step would be much slower and highly thermo-activated. The corresponding rate constant k_3 depends first on the lability of the hydrogen atom under consideration along the polymer chain (PH) and second, on the reactivity of the peroxy radical ($PO_2^{\bullet}$). Structure/property relationships are well known in this domain.[26]

In the case of EPDM terpolymers, oxidation can propagate through three different sites: secondary, tertiary, and allylic C–H bonds. These three sites are underlined in the repetitive monomer unit of Figure 1. Their reactivity can be expressed as

$$r_i = k_{3i}\left[PO_2^{\bullet}\right]\left[P_iH\right] \tag{1}$$

where index i refers to the type of C–H bond under consideration. For a sake of simplicity, let us denote secondary, tertiary, and allylic C–H bonds with indexes "s," "t," and "a," respectively. As an illustration, the probability that secondary C–H bonds are involved in the radical attack may be expressed as

$$p_s = \frac{r_s}{r_s + r_t + r_a} = \frac{k_{3s}[P_sH]}{k_{3s}[P_sH] + k_{3t}[P_tH] + k_{3a}[P_aH]} \tag{2}$$

Expressions of p_t and p_a can be obtained by circular permutation of indexes.

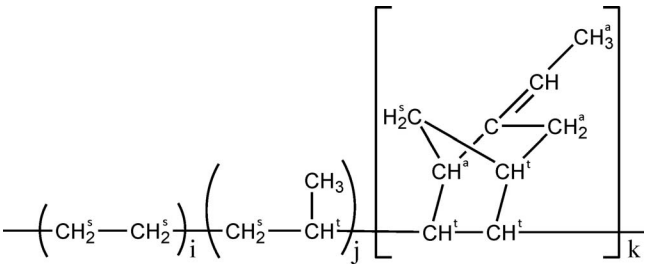


FIG. 1. — Chemical formula of an EPDM terpolymer having ethylidene norbornene (ENB) as diene monomer. Identification of the three reactive sites: (s) secondary, (t) tertiary and (a) allylic C–H bonds.

According to the literature,[27–29] whatever the temperature, allylic C–H bonds are about 10–50 times more reactive than the two other C–H bonds. However, in EPDM terpolymers, their molar fraction is too low (generally lower than 2 mol.%) to really play a significant role. As shown in Figure 2, for a commercial EPDM having an ethylene fraction typically higher than 60 mol.% and a propylene fraction lower than 40 mol.%, oxidation will preferentially propagate through secondary C–H bonds. In other words, such a polymer will behave like polyethylene (PE).

In the absence of antioxidants, termination is also the subject of a general consensus: it would result from the bimolecular termination of radicals and imply three distinct reactions (see Scheme 2). Since the alkyl radicals ($P^{\bullet}$) are considerably more reactive than $PO_2^{\bullet}$ radicals, the following classification is usually observed:[30] $k_4 > k_5 \gg k_6$.

The most delicate and controversial problem concerns initiation. Initiation reactions can be very diverse and complex: they vary with the polymer nature and aging temperature, but they all lead to the formation of $P^{\bullet}$ radicals. At low to moderate temperatures, it can be easily demonstrated that the production of radicals by polymer thermolysis is negligible.[31] In this case, the main source of radicals

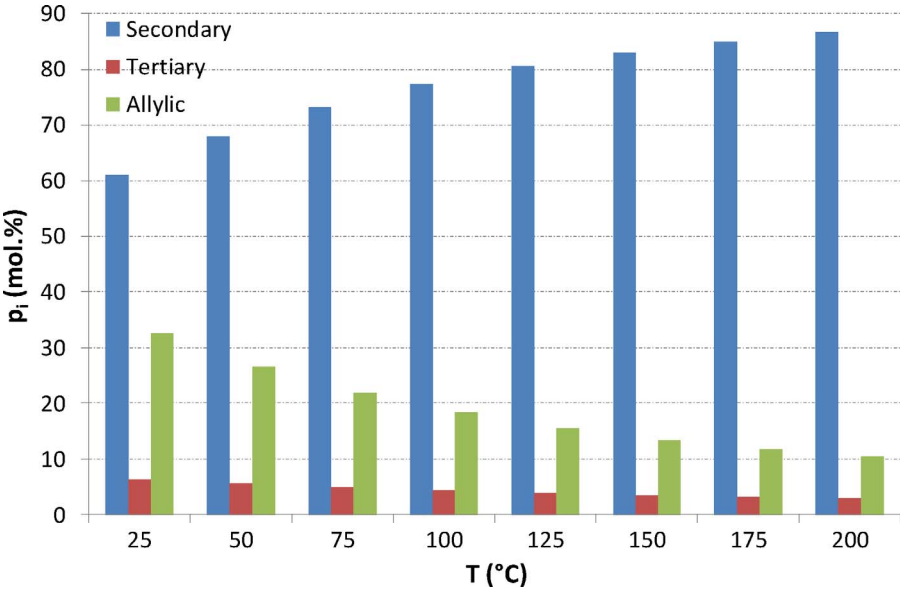


FIG. 2. — Probability for secondary, tertiary and allylic C–H bonds being involved in the radical attack between 25 and 200 °C. Results obtained for a commercial EPDM terpolymer referenced as Nordel 4570 and having an ethylene fraction of 62 mol.%, a propylene fraction of 36.6 mol.%, and an ENB fraction of 1.4 mol.%.

(4) $P^{\bullet} + P^{\bullet} \rightarrow \gamma_4 P\text{-}P + (1\text{-}\gamma_4)PH + (1\text{-}\gamma_4)F$ (k_4)
(5) $P^{\bullet} + PO_2^{\bullet} \rightarrow \gamma_5 POOP + (1\text{-}\gamma_5)POOH + (1\text{-}\gamma_5)F$ (k_5)
(6) $PO_2^{\bullet} + PO_2^{\bullet} \rightarrow$ inactive products + O_2 (k_6)

where F designates a double bond and γ_4 and γ_5 are chemical yields (lower than unity) accounting for the coupling efficiency of radical species and thus, $(1\text{-}\gamma_4)$ and $(1\text{-}\gamma_5)$ for the resulting efficiency of their disproportionation.

SCHEME 2. — Common termination steps.

is the thermal decomposition the most unstable species formed in propagation (see Scheme 1): the hydroperoxide POOH.[20] In other words, the thermal oxidation reaction produces its own initiator. This "closed-loop" character is responsible for the sharp auto-acceleration of the oxidation at the end of an induction period. POOH can decompose according to a unimolecular or bimolecular mode (see Scheme 3).

Layer 1: Non-terminating Bimolecular Combination. — In PE, it has been shown that the termination of $PO_2^{\bullet}$ radicals is not very efficient.[32] Indeed, at 45 °C, about 35–40% of pairs of alkoxy radicals ($PO^{\bullet}$) escape from the cage to initiate new oxidation chains. Thus, a more realistic writing of the bimolecular combination of $PO_2^{\bullet}$ radicals is given in Scheme 4. It involves three competitive reaction paths: coupling (6b), disproportionation (6c), and the rapid rearrangement of $PO^{\bullet}$ radicals outside the cage (6d).

Layer 2: Addition of Radicals onto Double Bonds. — In polyene elastomers, a second important source of propagation is the addition of radical species onto double bonds.[6–9] These two reactions are summarized in Scheme 5. In a first approach, they are considered exclusively intermolecular, although it is known that, in other types of elastomer (in particular in IR), they can be also intramolecular.[6–9]

Layer 3: Thermal Decomposition of Dialkyl Peroxide Bridges. — Reaction 7b leads to the formation of a large amount of dialkyl peroxide bridges (POOP) as unstable as POOH. Contrary to saturated hydrocarbon polymers, in the case of polyene elastomers, their contribution to initiation can no longer be neglected. Their thermal decomposition is exclusively unimolecular (see Scheme 6).

Layer 4: Stabilization by Hindered Phenols. — There are two main routes of stabilizing EPDM terpolymers against thermal oxidation:[33]

- Reducing the initiation rate by decomposing POOH by a non-radical way.
- Reducing the propagation rate (or increase the termination rate) by scavenging efficiently the radical species.

Hindered phenols and secondary aromatic amines belong to the second family of antioxidants.

Hindered phenols (AH) present two main features. First, they have a hydrogen atom much more labile than any hydrocarbon polymer. Indeed, in our case, the dissociation energy of their A–H bond is of the order of 335–355 kJ mol^{-1} against about 393 kJ mol^{-1} for secondary C–H bonds.[34–36] Thus, hindered phenols will easily give hydrogen to a $PO_2^{\bullet}$ radical. In addition, the resulting phenoxy radical ($A^{\bullet}$) is stabilized by resonance, that is, it transforms almost instantaneously into a radical quinonic structure ($B^{\bullet}$).

Second, radical $B^{\bullet}$ is not very reactive. It is often considered to be a stable species, unable to initiate new oxidation chains even when reactions are very complex, as they generally are.[37,38] In contrast, it can participate in a new stabilization event.[25,33,39] Finally, the action mechanism of hindered phenols could be summarized by Scheme 7.

(1u) POOH $\rightarrow 2P^{\bullet}$ + inact. prod. (k_{1u})
(1b) 2POOH $\rightarrow P^{\bullet} + PO_2^{\bullet}$ + inact. prod. (k_{1b})

SCHEME 3. — Thermal decomposition of hydroperoxides.

(6a) $PO_2^\bullet + PO_2^\bullet$	$\rightarrow [PO^\bullet\ {}^\bullet OP]_{cage} + O_2$	(k_{6a})
(6b) $[PO^\bullet\ {}^\bullet OP]_{cage}$	$\rightarrow$ POOP	(k_{6b})
(6c) $[PO^\bullet\ {}^\bullet OP]_{cage}$	$\rightarrow$ P=O + P-OH	(k_{6c})
(6d) $[PO^\bullet\ {}^\bullet OP]_{cage}$	$\rightarrow 2P^\bullet$ + inact. prod.	(k_{6d})

where $[PO^\bullet\ {}^\bullet OP]_{cage}$ designates a pair of caged alkoxy radicals.

SCHEME 4. — Bimolecular combination of peroxy radicals.

Layer 5: Stabilization by Hindered Amines. — Contrary to hindered phenols, the action mechanism of hindered amines is still controversial because of its high complexity. The active species is a free radical, namely, the nitroxy radical (>NO$^\bullet$), which can be directly incorporated into the polymer matrix during the processing operation or be formed by oxidation of hindered amine (>NH) in the early periods of exposure.[40,41]

There is a relative consensus on the fact that >NO$^\bullet$ radicals are unable to initiate new oxidation reactions, but efficiently scavenge P$^\bullet$ radicals in order to form an alkoxy amine (>NOP).[42,43] In addition, >NO$^\bullet$ radicals would be regenerated according to a two-step reaction: >NOP would decompose into hydroxyl amine (>NOH) that would then react with $PO_2^\bullet$ radicals to give a >NO$^\bullet$ radical and a POOH.[44,45] This two-step reaction is usually written in the form of a balance reaction. The action mechanism of hindered amines is summarized by Scheme 8.

The regeneration cycle composed of the two reactions 14 and 15 is commonly called the "Denisov cycle."

Layer 6: Stabilization by Sulfide Bridges. — It is well known that sulfide bridges (especially monosulfide and disulfide bridges) decompose POOH in a non-radical way.[46–48] More generally, sulfide bridges (P_2S) can progressively be transformed into sulfur structures with an increasing degree of oxidation (see Scheme 9): First, in sulfoxide (P_2SO) and sulfenic acid (PSOH), then in sulfone (P_2SO_2) and sulfinic acid (PSO_2H), then in sulfonic acid (PSO_3H), and finally in sulfuric acid (SO_4H_2). This series of consecutive transformations delays and slows down the oxidation reaction, particularly when comparing sulfur vulcanized elastomers with their starting linear polymer.[49] In addition, it involves the breaking of C–S bonds, that is, the destruction of cross-link nodes.

For the sake of simplicity, it was decided to distinguish the action of sulfur from the action of its oxidation products, that is, to consider the two reactions in Scheme 10.

Layer 7: Concentration of Oxidation Products. — The general mechanistic scheme composed of reactions 1u to 17 was used to describe the thermal oxidation of a stabilized and sulfur vulcanized EPDM. A system of 17 non-linear differential equations (one equation per reactive species) was derived from this mechanistic scheme using the classical rules of the chemical kinetics (see Appendix A). The numerical solution of this system, with algorithms especially recommended for "stiff problems" of chemical kinetics, has been reported in many papers, for instance in Colin et al.[30] This solution gives access to the concentration changes over time of all the reactive species, that is, POOH, POOP, P$^\bullet$, $PO_2^\bullet$, $[PO^\bullet\ {}^\bullet OP]_{cage}$, PH, F_{ENB}, AH, B$^\bullet$, >NH, >N$^\bullet$, >NO$_2^\bullet$, >NO$^\bullet$, >NOP, P_2S, PSO_iR, and C–S.

From these primary quantities, an important number of secondary quantities can be calculated, in particular molecular quantities that are accessible experimentally and, thus, can be used to validate the system of differential equations. The most reliable quantity is undoubtedly oxygen

(7a) $P^\bullet + F_{ENB}$	$\rightarrow$ P-P + P$^\bullet$	(k_{7a})
(7b) $PO_2^\bullet + F_{ENB}$	$\rightarrow$ POOP + P$^\bullet$	(k_{7b})

where F_{ENB} designates an ethylidene double bond.

SCHEME 5. — Propagation by addition of radicals onto double bonds.

(1p) POOP $\rightarrow$ $2P^{\bullet}$ + inact. prod. (k_{1b})

SCHEME 6. — Thermal decomposition of dialkyl peroxides.

absorption, since its calculation does not require the use of additional hypotheses or adjustable parameters (except rate constants):

$$\left.\frac{d[O_2]}{dt}\right|_{Abs} = k_2[P^{\bullet}][O_2] - k_{6a}\left[PO_2^{\bullet}\right]^2 + k_{10}[O_2][>NH] + k_{12}[>N^{\bullet}][O_2] - k_{13}\left[>NO_2^{\bullet}\right]^2 \quad (3)$$

Other molecular quantities, where calculation requires the use of formation yields, are the concentrations of the different oxidation products. As an example, carbonyl species (i.e., ketones, aldehydes, carboxylic acids, esters, etc.) are formed in reactions 1u, 1b, 1p, 6c, and 6d. Thus, their global concentration may be expressed as

$$\frac{d[P=O]}{dt} = \gamma_1 k_{1u}[POOH] + \gamma_1 k_{1b}[POOH]^2 + 2\gamma_1 k_{1p}[POOP] + k_{6c}[PO^{\bullet\bullet}OP]_{cage} + 2\gamma_1 k_{6d}[PO^{\bullet\bullet}OP]_{cage} \quad (4)$$

Let us remark that the formation yield γ_1 is identical in reactions 1u, 1b, 1p, and 6d, because carbonyls are formed by the rapid rearrangement (by β scission) of the same $PO^{\bullet}$ radical.

Layer 8: Weight Changes. — During its thermal exposure, the polymer consumes oxygen and releases many volatile compounds such as water and other small molecules formed by the rapid rearrangement (by β scission) of $PO^{\bullet}$ radicals near the chain extremities in reactions 1u, 1b, 1p, and 6d. For the sake of simplicity, these latter molecules have been assimilated to a single "average" molecule noted *V*, of molar mass M_V and formed with a yield υ. Thus, the balance equation between weight uptake (due to oxygen absorption) and weight loss (due to emission of volatile compounds) may be written as

$$\frac{1}{m_0}\frac{dm}{dt} = \frac{32}{\rho_0}\left\{k_2[P^{\bullet}][O_2] - k_{6a}\left[PO_2^{\bullet}\right]^2 + k_{10}[O_2][>NH] + k_{12}[>N^{\bullet}][O_2] - k_{13}\left[>NO_2^{\bullet}\right]^2\right\} - \frac{18+\upsilon M_V}{\rho_0}\left\{k_{1u}[POOH] + k_{1b}[POOH]^2\right\} - \frac{2\upsilon M_V}{\rho_0}\left\{k_{1p}[POOP] + k_{6d}[PO^{\bullet\bullet}OP]_{cage}\right\} \quad (5)$$

where ρ_0 is the initial polymer density.

Layer 9: Maturation and Reversion. — It is also well known that polysulfides bridges, formed during the vulcanization process, are thermally unstable.[50,51] Their thermal decomposition leads to the formation of shorter and, thus, more stable (disulfide and monosulfide) bridges. However, this maturation (or post-cross-linking) can be totally supplanted by reversion when increasing the temperature.[21,50,51]

Maturation/reversion phenomena are very difficult to model accurately because of the great variety of polysulfide bridges[48] and the large number of possible elementary reactions.[52] However, it is possible to give a satisfactory description of their fate at the macromolecular level with a simplified mechanistic scheme (see Scheme 11) composed of only three virtual chemical species: a post-cross-linking precursor (Prec), a stable sulfide bridge (X_S) and an unstable sulfide bridge

(8) AH + $PO_2^{\bullet}$ $\rightarrow$ $B^{\bullet}$ + POOH (k_8)
(9) $B^{\bullet}$ + $PO_2^{\bullet}$ $\rightarrow$ inact. prod. (k_9)

SCHEME 7. — Simplified mechanism of stabilization by hindered phenols.

(10) O_2 + >NH	→ >N$^\bullet$	(k_{10})
(11) $PO_2^\bullet$ + >NH	→ POOH + >N$^\bullet$	(k_{11})
(12) >N$^\bullet$ + O_2	→ >$NO_2^\bullet$	(k_{12})
(13) >$NO_2^\bullet$ + >$NO_2^\bullet$	→ >NO$^\bullet$ + >NO$^\bullet$ + O_2	(k_{13})
(14) >NO$^\bullet$ + P$^\bullet$	→ >NOP	(k_{14})
(15) $PO_2^\bullet$ + >NOP	→ POOH + >NO$^\bullet$ + F	(k_{15})

SCHEME 8. — Realistic mechanism of stabilization by hindered amines.

(X_U). Such a scheme was found to be successful in predicting the changes in elastic modulus of sulfur vulcanized IR.[21]

A system of three linear differential equations (one equation per chemical species) was derived from this mechanistic scheme using the classical rules of chemical kinetics (see Appendix B). The numerical solution of this system with the same algorithm is given in Appendix A. This approach allows access to the concentration changes over time of the three chemical species, that is, Prec, X_S, and X_U.

Layer 10: Damage Mechanisms. — Chain scission and cross-linking events are responsible for the changes in macromolecular structure. Their respective concentration can also be deduced from the primary molecular quantities. Chain scissions *S* derive essentially from the rapid rearrangement (by β scission) of PO$^\bullet$ radicals in other places besides the chain extremities in reactions 1u, 1b, 1p, and 6d. Thus, their concentration may be expressed as

$$\frac{dS}{dt} = \gamma_S k_{1u}[\mathrm{POOH}] + \gamma_S k_{1b}[\mathrm{POOH}]^2 + 2\gamma_S k_{1p}[\mathrm{POOP}] + 2\gamma_S k_{6d}[\mathrm{PO^{\bullet\bullet}OP}]_{\mathrm{cage}} \qquad (6)$$

where γ_S is the yield in chain scissions in the reactions under consideration.

In contrast, cross-linking X arises from the coupling of radical species in reactions 4, 5, and 6b, the addition of radical species onto ethylidene double bonds in reactions 7a and 7b, and maturation 18. However, recall that de-cross-linking events occur in initiation 1p, stabilization reactions 16 and 17 by sulfur bridges, and reversion 19. Finally, the total concentration of cross-linking events may be written as

$$\begin{aligned}\frac{dX}{dt} = &-k_{1p}[\mathrm{POOP}] \\ &+ \gamma_4 k_4[\mathrm{P^\bullet}]^2 + \gamma_5 k_5[\mathrm{P^\bullet}]\left[\mathrm{PO_2^\bullet}\right] \\ &+ k_{6b}[\mathrm{PO^{\bullet\bullet}OP}]_{\mathrm{cage}} + k_{7a}[\mathrm{P^\bullet}][F_{\mathrm{ENB}}] + k_{7b}\left[\mathrm{PO_2^\bullet}\right][F_{\mathrm{ENB}}] - \gamma_{16}k_{16}[\mathrm{P_2S}][\mathrm{POOH}] \\ &- (1+\gamma_{17})k_{17}[\mathrm{PSO_iR}][\mathrm{POOH}] + k_{18}[\mathrm{Prec}] - k_{19}X_U \end{aligned} \qquad (7)$$

where γ_4 and γ_5 are the respective coupling yields of radical species in termination reactions 4 and 5, and γ_{16} and γ_{17} are the respective breaking yields of C–S bonds, according to the Colclough's mechanism,[47] in reactions 16 and 17.

P_2S + POOH	→ ξP_2SO + (1-ξ)PSOH	- (1-ξ)C-S
PSOH + POOH	→ PSO_2H	
P_2SO + POOH	→ $\xi' P_2SO_2$ + (1-ξ')PSO_2H	- (1-ξ')C-S
PSO_2H + POOH	→ PSO_3H	
PSO_3H + POOH	→ SO_4H_2	- C-S

where C-S designates a carbon-sulfur bond and (1-ξ) and (1-ξ') are chemical yields (lower than unity) accounting for the efficiency of the Colclough's mechanism[47] in the elementary reactions under consideration, that involves the breaking of a C-S bond.

SCHEME 9. — Realistic mechanism of stabilization by sulfur bridges.

(16) $P_2S + POOH$	$\rightarrow$ PSOR	$-\gamma_{16}$C-S	(k_{16})
(17) $PSO_iR + 4POOH$	$\rightarrow PSO_{i+1}R$	$-(1+\gamma_{17})$C-S	(k_{17})

where R designates a polymer chain (P) or an hydrogen atom (H), and i is an index varying from 1 to 3. Note that the efficiency of the Colclough's mechanism[47] is now accounted by using global chemical yields γ_{16} and $(1+\gamma_{17})$.

SCHEME 10. — Simplified mechanism of stabilization by sulfur bridges.

Layer 11: Macromolecular Changes. — Knowing S and X, the changes in the macromolecular structure can be now calculated. For linear polymers (e.g., for the starting linear EPDM), S and X are linked to the average molar masses according to the Saito's equations:[53,54]

$$S - X = \frac{1}{M_n} - \frac{1}{M_{n0}} \tag{8}$$

$$\frac{S}{2} - 2X = \frac{1}{M_W} - \frac{1}{M_{W0}} \tag{9}$$

where M_{n0}, M_n, M_{W0}, and M_W are the number and weight average molecular masses before and after thermal exposure, respectively, that is,

$$M_n = \frac{M_{n0}}{1 + M_{n0}(S - X)} \tag{10}$$

$$M_W = \frac{2M_{W0}}{2 + M_{W0}(S - 4X)} \tag{11}$$

In contrast, for elastomer networks, S and X are linked to the concentrations of elastically active chains, between two consecutive cross-link nodes, and dangling chains. Since nodes are tetrafunctional, each chain scission suppresses one elastically active chain, creates two dangling chains, and transforms two tetrafunctional nodes into trifunctional nodes (see Figure 3a). In contrast, each cross-linking event creates two new elastically active chains and one tetrafunctional node (see Figure 3b). It may be thus written as

$$\nu = \nu_0 - S + 2X \tag{12}$$

$$b = b_0 + 2S \tag{13}$$

$$n = n_0 + X \tag{14}$$

where ν_0, ν, b_0, b, n_0, and n are the concentrations in elastically active chains, dangling chains, and cross-link nodes before and after thermal exposure, respectively. Recall that the initial concentration in dangling chains is in fact the concentration in chain extremities of the starting linear polymer, that is,

$$b_0 = \frac{2}{M_{n0}} \tag{15}$$

(18) Prec	$\rightarrow \gamma_{18}X_S + (1-\gamma_{18})X_U$	(k_{18})
(19) X_U	$\rightarrow$ non-crosslinking products	(k_{19})

where γ_{18} is a "partition coefficient" between stable and unstable sulfide bridges.

SCHEME 11. — Simplified mechanism of maturation/reversion.

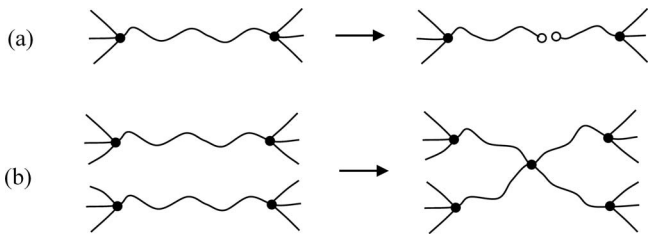


FIG. 3. — (a) Schematic chain scission and (b) cross-linking event in an elastomer network.

In addition, for initially almost perfect networks (for which $b_0 \ll \nu_0$), it may be written as

$$n_0 = \frac{2}{f}\nu_0 \tag{16}$$

$$M_{C0} = \frac{1}{\nu_0} \tag{17}$$

where f is the functionality of cross-link nodes.

If this network is subjected to a largely predominant cross-linking process, the average molar mass between two consecutive cross-link nodes decreases with time of exposure. In this case, Eq. 17 remains valid whatever the time of exposure:

$$M_C = \frac{1}{\nu} \tag{18}$$

MECHANICAL LEVEL

In a first approach, the "mechanical level" has been derived from a modified version of the statistical theory of rubber elasticity, called the phantom network theory.[55] This theory considers a perfect network and an affine deformation and takes into account the fluctuation of cross-link nodes around their equilibrium position. According to this theory, in uniaxial tension, it may be written as

$$\sigma = \frac{\rho R T}{M_C}\left(1 - \frac{2}{f}\right)\left(\lambda^2 - \frac{1}{\lambda}\right) \tag{19}$$

where σ and λ are the true stress and extension ratio in the loading direction, respectively; ρ the polymer density; R the universal constant of perfect gas ($R = 8.314$ J mol^{-1} K^{-1}); and T the absolute temperature.

Equation 19 allows capturing the mechanical response in tension of the elastomer material up to its breaking point of coordinates (σ_b, λ_b). Indeed, σ_b is linked to λ_b according to Eq. 19. In general, the expression of λ_b is determined by assuming that the rupture occurs when the elastically active chains reach their maximum extension and by taking into account the chain tortuosity.[56] After having performed several suitable transformations, the following general rupture criterion may be proposed:

$$\frac{\lambda_b - 1}{\lambda_{b0} - 1} = \left(\frac{M_C - M_{CY}}{M_{C0} - M_{CY}}\right)^{\alpha} \tag{20}$$

where λ_{b0}, λ_b, M_{C0}, and M_C are the extension ratio at break and the average molar mass

TABLE I
CHARACTERISTICS OF COMMERCIAL EPDM TERPOLYMERS USED IN THIS STUDY

EPDM	Ethylene (mol.%)	Propylene (mol.%)	ENB (mol.%)
Nordel IP3745P	78.0	21.9	0.1
ND*	67.4	31.6	1.0
Nordel 4640	66.2	32.5	1.4
Nordel 4520	62.8	36.1	1.2
Nordel 4570	62.0	36.6	1.4

* ND = Not disclosed

between two consecutive cross-link nodes before and after thermal exposure, respectively. M_{CY} would be the average molar mass of the completely degraded network, and α a constant close to unity.

Finally, the complete mechanical response in tension of the elastomer material can be described by slightly modifying Eq. 19 as follows:

$$\sigma = \frac{\rho R T}{M_C}\left(1 - \frac{2}{f}\right)\left(\lambda^2 - \frac{1}{\lambda}\right)F(M_C) \tag{21}$$

where $F(M_C)$ is modified sigmoid (s-shaped) function satisfying the following conditions:

- $F = 1$ if $\lambda < \lambda_b$
- $F \to 0$ if $\lambda \geq \lambda_b$

and the input parameters being M_{C0}, M_{CY}, and λ_{b0}.

RESULTS AND DISCUSSION

A heavy thermal aging campaign was carried out in air-ventilated ovens between 70 and 170 °C on press-molded samples (films and plates) obtained from four distinct EPDM formulations: additive free gum, unstabilized and stabilized sulfur vulcanized gum, and industrial material. The chemical characteristics of the different commercial EPDM terpolymers used in this study are delineated in Table I. All these linear EPDMs have an ethylene fraction typically higher than 60 mol.% and a propylene fraction lower than 40 mol.%. Their thermal oxidation behavior is thus expected to be very close to PE.

After thermal aging, a multiplicity of analytical techniques was employed for characterizing the structural changes occurring at the molecular level (antioxidants, carbonyl products, double bonds, and sulfide bridges), as well as at the macromolecular (chain scissions and cross-link nodes) and macroscopic levels (weight changes). Stress–strain measurements were conducted to investigate the influence of thermal aging mechanisms on the elastic and fracture properties. The collective experimental results were used to quantify the multitude of parameters and, thus, to check the validity of the chemo-mechanical model. In this section, only a few examples of simulations are reported to illustrate the reliability of the model. The examples given here relate specifically to EPDM, designated not disclosed (ND) in Table I. Because we are bound by confidentiality, the commercial reference of this grade of EPDM cannot be divulged. However, for the purposes of this study, no restriction was imposed upon us in determining the structural characteristics of this particular grade of EPDM (see Table II).

TABLE II
STRUCTURAL CHARACTERISTICS OF EPDM RUBBERS USED IN THIS STUDY

	Free additive gum	Unstabilized sulfur vulcanized gum	Stabilized sulfur vulcanized gum	Industrial material
Chemical characteristics				
$[POOH]_0$ (mol L^{-1})	10^{-4}	10^{-5}	10^{-5}	10^{-5}
$[PH]_0$ (mol L^{-1})	29.1	29.1	29.1	29.1
$[F_{ENB}]_0$ (mol L^{-1})	1.7×10^{-1}	8.0×10^{-2}	8.0×10^{-2}	8.0×10^{-2}
$[AH]_0$ (mol L^{-1})	—	—	—	—
$[>NH]_0$ (mol L^{-1})	—	—	5.0×10^{-2}	5.0×10^{-2}
$[C–S]_0$ (mol L^{-1})	—	5.5×10^{-1}	5.2×10^{-1}	—
$[P_2S]_0$ (mol L^{-1})	—	4.0×10^{-1}	4.0×10^{-1}	4.0×10^{-1}
$[Prec]_0$ (mol L^{-1})	—	—	1.5×10^{-1}	1.5×10^{-1}
Physical characteristics				
M_{n0} (g mol^{-1})	109,000	—	—	—
M_{W0} (g mol^{-1})	234,000	—	—	—
ν_0 (mol L^{-1})	—	2.8×10^{-1}	2.6×10^{-1}	4.8×10^{-1}
b_0 (mol L^{-1})	—	9.2×10^{-6}	9.2×10^{-6}	9.2×10^{-6}
n_0 (mol L^{-1})	—	1.4×10^{-1}	1.3×10^{-1}	2.4×10^{-1}
M_{C0} (g mol^{-1})	—	3127	3282	1780

As a first example, the experimental data obtained on thin films of the additive free EPDM gum are given in Figures 4 to 7. It should be noted that the films were chosen to be thin enough (typically between 20 and 150 μm) to avoid any diffusion control of oxidation. A good agreement between theory and experimental results is obtained irrespective of the temperature and aging marker under consideration. Difficulties were encountered when attempting to determine by gel permeation chromatography (GPC) the changes in molar masses in the early periods of exposure. Presumably, this difficulty was caused by cross-linking reactions predominating over chain scissions and thereby preventing the complete dissolution of the polymer in 1,2,4-trichlorobenzene at 160 °C. However, over longer periods, dissolution occurs relatively easily, thus allowing for untrammeled characterization of the polymer (see Figure 6).

The reasonably accurate simulation of all experimental data permitted the determination of all 13 rate constants at the "chemical level." As expected, the Arrhenius law is obeyed over the whole range of temperatures used in this study (between 70 and 170 °C). The corresponding Arrhenius parameters are given in Table III. They call for the following comments:

- As expected, almost all the rate constants (from k_{1u} to k_{6d}) give similar values for EPDM and PE.[27,57–59] In addition, a comparatively small difference is observed between the values of constant k_3, for which the pre-exponential factor is about six times greater and the activation energy is about 5 kJ mol^{-1} greater for EPDM, no doubt because of the presence of allylic and tertiary C–H bonds in EPDM, which are believed to be more reactive than secondary C–H bonds. This small difference fully justifies the first assumption in the "chemical level": EPDM terpolymers with an ethylene fraction higher than 60 mol.% behave like PE.
- In EPDM terpolymers, the concentration of ethylidene double bonds is clearly too low (see Table I) to affect the global oxidation kinetics. Indeed, oxidation propagates essentially by

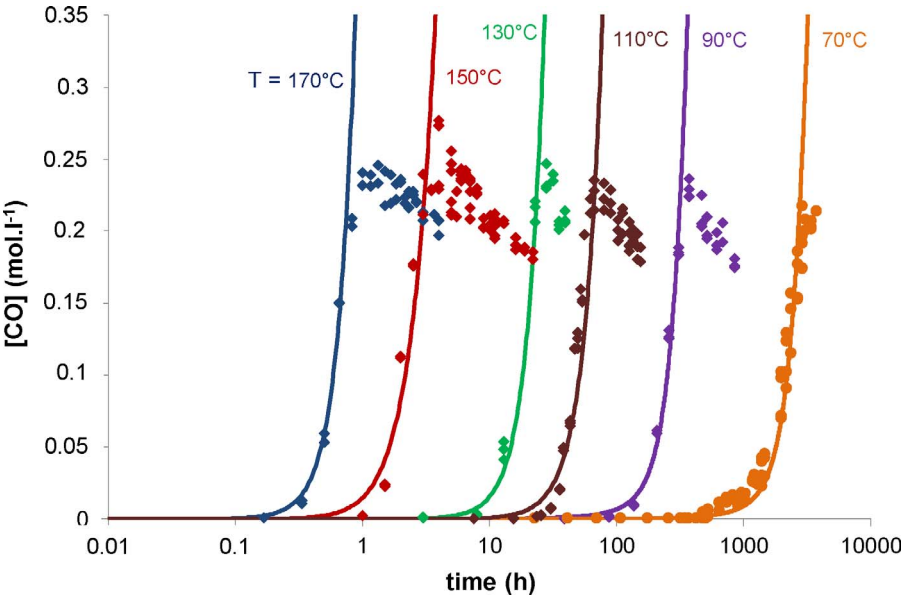


FIG. 4. — Modeling (continuous lines) of carbonyl build-up (symbols) in air between 70 and 170 °C for an additive free EPDM gum. Experimental concentrations determined by the Beer–Lambert's law from the IR absorption band of carbonyl groups at 1715 cm^{-1} and taking an average value for the coefficient of molar extinction of 460 L mol^{-1} cm^{-1}.

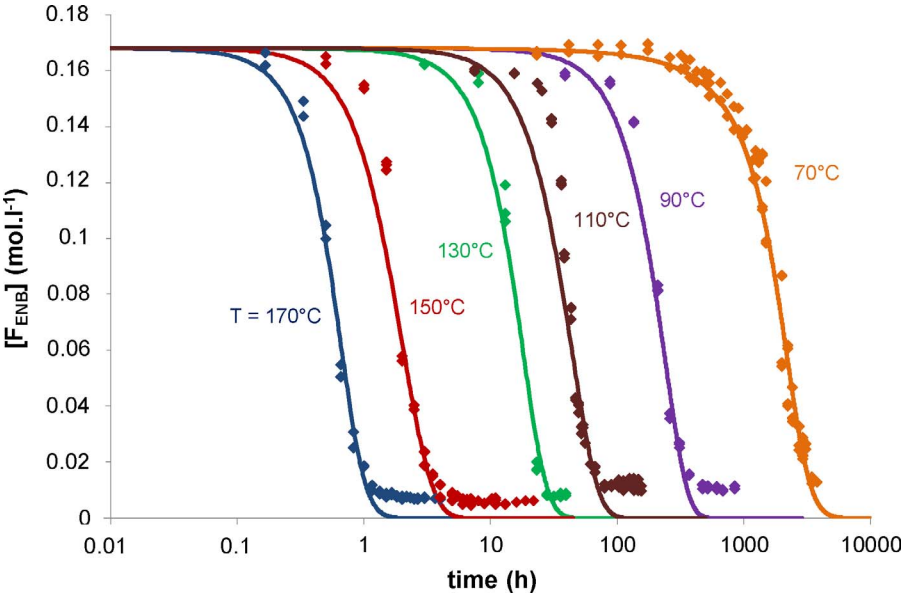


FIG. 5. — Modeling (continuous lines) of the consumption of ethylidene double bonds (symbols) in air between 70 and 170 °C for an additive free EPDM gum. Experimental concentrations determined by the Beer–Lambert's law from the IR absorption band of ethylidene double bonds at 809 cm^{-1} and taking an average value for the coefficient of molar extinction of 40 L mol^{-1} cm^{-1}.

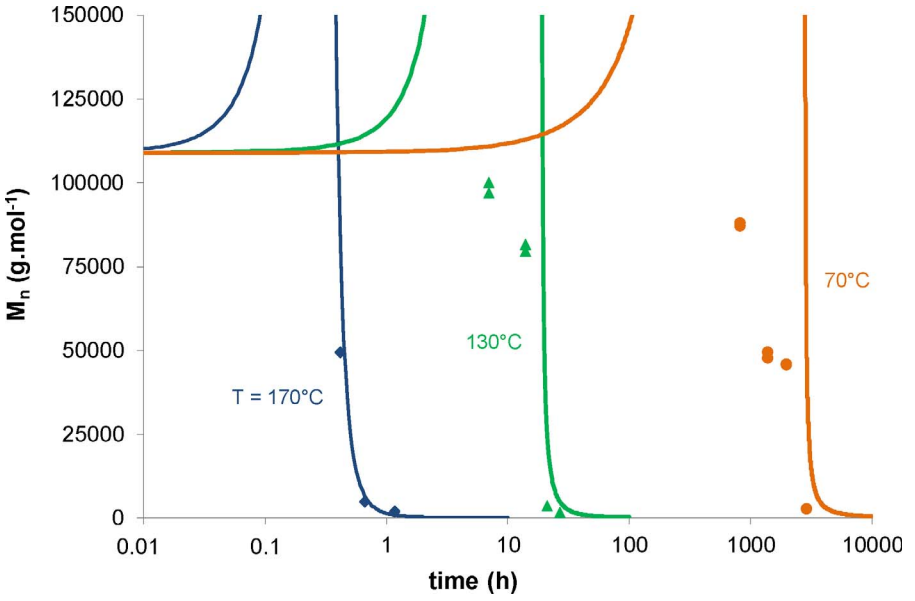


FIG. 6. — Modeling (continuous lines) of the changes in the number average molar masses (symbols) in air between 70 and 170 °C for an additive free EPDM gum. Experimental data obtained by size exclusion chromatography (gel permeation chromatography) at 160 °C using 1,2,4-trichlorobenzene as eluent, and after correction by the so-called "universal calibration" method.

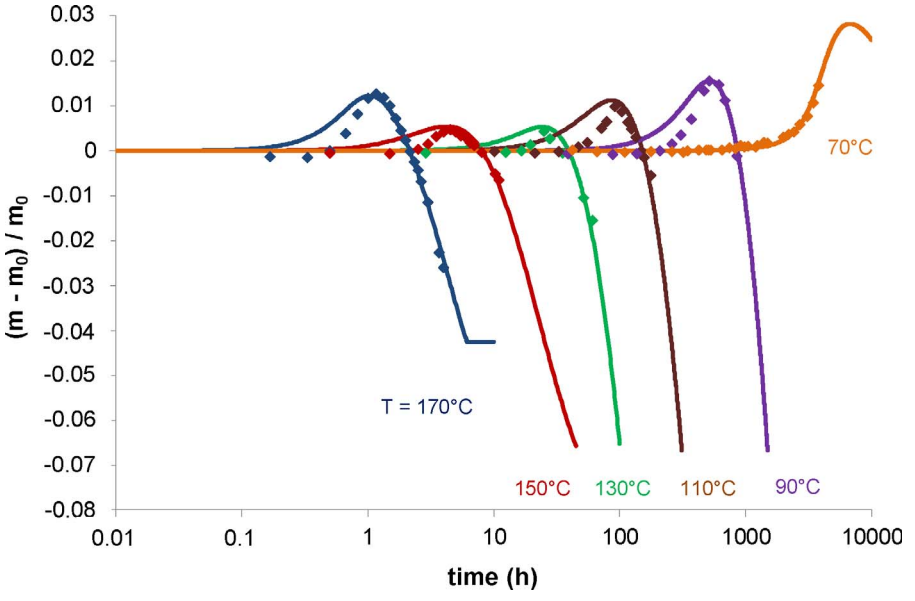


FIG. 7. — Modeling (continuous lines) of weight changes (symbols) in air between 70 and 170 °C for an additive free EPDM gum. Experimental data obtained by periodically weighting the samples on a standard laboratory microbalance.

TABLE III
ARRHENIUS PARAMETERS BETWEEN 70 AND 170 °C USED FOR THE SIMULATION OF THE KINETIC CURVES GIVEN IN FIGURES 4 TO 7 FOR ADDITIVE FREE EPDM GUM

Kinetic parameter	Pre-exponential factor	Activation energy (kJ mol^{-1})
$[O_2]_0$ (mol L^{-1})	8.4×10^{-4}	0
k_{1u} (s^{-1})	8.0×10^{12}	140
k_{1b} (L mol^{-1} s^{-1})	2.8×10^{9}	105
k_{1p} (L mol^{-1} s^{-1})	9.7×10^{11}	129
k_2 (L mol^{-1} s^{-1})	10^{8}	0
k_3 (L mol^{-1} s^{-1})	9.9×10^{10}	78
k_4 (L mol^{-1} s^{-1})	8.0×10^{11}	0
k_5 (L mol^{-1} s^{-1})	2.3×10^{11}	0
k_{6a} (L mol^{-1} s^{-1})	4.9×10^{19}	80
k_{6b} (s^{-1})	2.0×10^{6}	0
k_{6c} (s^{-1})	1.2×10^{6}	5
k_{6d} (s^{-1})	8.0×10^{12}	50
k_{7a} (L mol^{-1} s^{-1})	1.9×10^{6}	8
k_{7b} (L mol^{-1} s^{-1})	1.8×10^{11}	67
γ_1 (%)	60–90	—
γ_S (%)	100	—
γ_4 (%)	0	—
γ_5 (%)	0	—
υM_V (g mol^{-1})	20–33	—

hydrogen abstraction through secondary C–H bonds, as in PE. However, it is crucial to maintain the addition of radical species onto double bonds in the final mechanistic scheme in order to explain why EPDM terpolymers are much more sensitive to cross-linking compared with PE (see Figure 6). Recall that, like chain scissions, cross-linking will also alter the mechanical properties and, therefore, influence the lifetime of any given elastomer.

- The decomposition of POOP bridges (1p) clearly provides a negligible contribution to initiation in the early periods of exposure. However, owing to the accumulation of POOP, the corresponding rate progressively increases with time of exposure. Therefore, the decomposition of POOP becomes increasingly significant and cannot be ignored over prolonged periods of time.

As a second example, the oxidation induction times determined by differential scanning calorimetry (DSC) at high temperature (typically between 170 and 200 °C) under a pure oxygen flow for the four distinct EPDM formulations are given in Table IV. Sulfide bridges markedly stabilize the EPDM gum against oxidation. Indeed, the oxidation induction time increases by a multiple factor of about 60 when comparing additive free and sulfur vulcanized gums. In contrast, the effects of the hindered amine antioxidant (1 wt% of 2,2,4-trimethyl-1,2-dihydroquinoline) and fillers (13 wt% of carbon black) are much weaker. Indeed, the oxidation induction time increases only by factors of about 3 and 1.2 when comparing the unstabilized and stabilized sulfur vulcanized gums and the industrial material. Thus, in a first approach, the stabilizing effects of antioxidant and carbon black could be neglected.

TABLE IV
COMPARISON OF THE OXIDATION INDUCTION TIMES (IN HOURS) IN PURE OXYGEN BETWEEN 170 AND 200 °C OF EPDM RUBBERS USED IN THIS STUDY

T (°C)	Free additive gum	Unstabilized sulfur vulcanized gum	Stabilized sulfur vulcanized gum	Industrial material
170	0.41	24.7	59.1	77.5
180	0.2	11.6	29.8	36
190	0	4.8	14.9	17.3
200	0	1.9	7.4	8.4

It should be noted the stabilization by sulfide bridges involves the progressive oxidation of sulfur atoms and, thus, the breaking of C–S bonds (see Scheme 9). As a third example, the concentration changes in C–S bonds of thin films of EPDM containing unstable sulfur are considered in Figure 8. Here also, the films were chosen thin enough (typically between 140 and 145 μm) to avoid any diffusion control of oxidation. Here again, a reasonable correlation is observed between theory and experiment, irrespective of the chosen exposure temperature.

The reasonably accurate simulation of these latter experimental data makes it possible to determine the two stabilization rate constants k_{16} and k_{17}. As expected, they obey also an Arrhenius law over the whole temperature range under investigation, that is, between 90 and 170 °C. Their corresponding Arrhenius parameters are given in Table V. These values are marginally lower than those reported in the literature for sulfur vulcanized IR.[49] Unfortunately, valid structure/property relationships cannot be given at this stage owing to the paucity of information in the literature based around this subject matter.

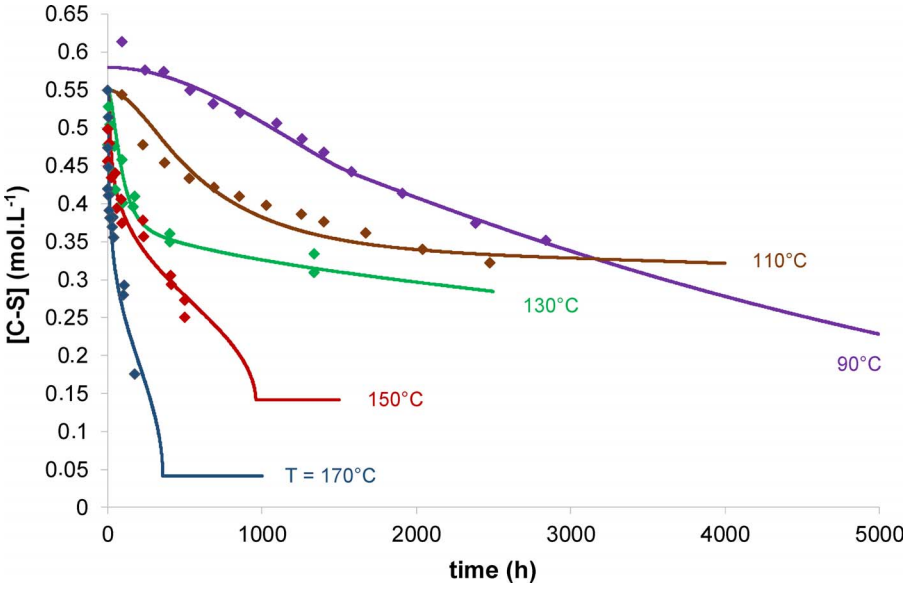


FIG. 8. — Modeling (continuous lines) of the depletion of carbon–sulfur bonds (symbols) in air between 90 and 170 °C for an unstabilized sulfur vulcanized EPDM gum. Experimental concentrations determined by the Beer–Lambert's law from the IR absorption band of carbon–sulfur bonds at 750 cm^{-1} and taking an average value for the coefficient of molar extinction of 70 L mol^{-1} cm^{-1}.

TABLE V
ARRHENIUS PARAMETERS BETWEEN 90 AND 170 °C USED FOR THE SIMULATION OF THE KINETIC CURVES GIVEN IN FIGURES 8 TO 10 FOR SULFUR VULCANIZED EPDM GUM

Kinetic parameter	Pre-exponential factor	Activation energy (kJ mol^{-1})
k_{16} (L mol^{-1} s^{-1})	2.1×10^5	44
k_{17} (L mol^{-1} s^{-1})	4.1×10^{11}	102
k_{18} (s^{-1})	1.1×10^1	60
γ_{16} (%)	10–41	—
γ_{17} (%)	51–100	—

As a fourth example, the changes in the macromolecular network (ν and M_C) measured by swelling in cyclohexane at room temperature on thick test pieces (typically 3.8 mm thick) for the stabilized sulfur vulcanized gum are given in Figures 9 and 10. Maturation (i.e., post-vulcanization) predominates largely over the oxidation reaction (i.e., cross-linking followed by chain scissions) of the EPDM chains.

The experimental data were used to determine the maturation rate constant k_{18}. As expected, this latter also obeys an Arrhenius law between 130 and 170 °C. The values of other associated parameters are given in Table V. These values are about one decade higher than those reported in the literature for sulfur vulcanized IR.[21] Here again, structure/property relationships cannot be cited owing to the lack of information in the literature.

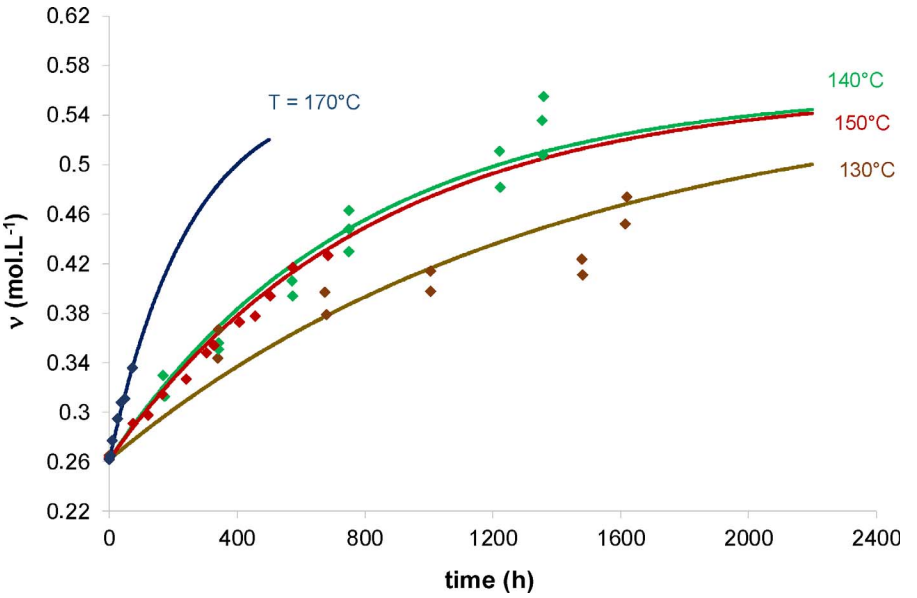


FIG. 9. — Modeling (continuous lines) of the concentration changes of elastically active chains (symbols) in air between 130 and 170 °C for a stabilized sulfur vulcanized EPDM gum. Experimental data determined by swelling test in cyclohexane at room temperature.

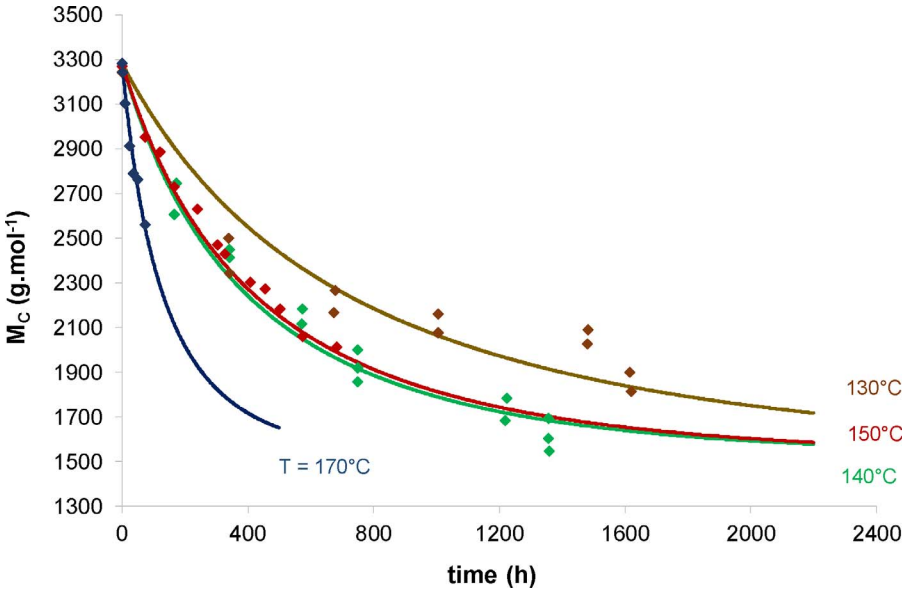


FIG. 10. — Modeling (continuous lines) of the changes in average mass between two consecutive cross-links (symbols) in air between 130 and 170 °C for a stabilized sulfur vulcanized EPDM gum. Experimental data determined by swelling test in cyclohexane at room temperature.

The final part of this work uses the calculated M_C values to predict the stress–strain behavior in tension of the industrial EPDM after thermal aging between 130 and 170 °C. In this endeavor, values given in Table VI were used.

Figure 11 indicates that a good agreement is obtained between the experimental results and those predicted by the stress–strain model (Eq. 21 in the text) over various durations of aging at 170 °C. This last check allows us to definitively conclude on the reliability of the chemo-mechanical model.

CONCLUSION AND PROSPECTS

A chemo-mechanical model has been developed for predicting the lifetime of EPDM rubbers in a harsh thermal oxidative environment. This model allows access to the structural changes occurring within the elastomeric network at the different relevant scales (molecular, macromolecular, and macroscopic scales) and the resulting changes in its mechanical response in tension. Its validity has been successfully checked over a large temperature range (typically between 70 and 170 °C) on four distinct EPDM formulations.

TABLE VI
PARAMETERS USED FOR PREDICTING THE MECHANICAL BEHAVIOR IN TENSION OF THE INDUSTRIAL MATERIAL AFTER THERMAL AGING IN AIR BETWEEN 130 AND 170 °C (SEE FIGURE 11)

M_{C0} (g mol^{-1})	M_{C0Y} (g mol^{-1})	α
1780	600	1.5

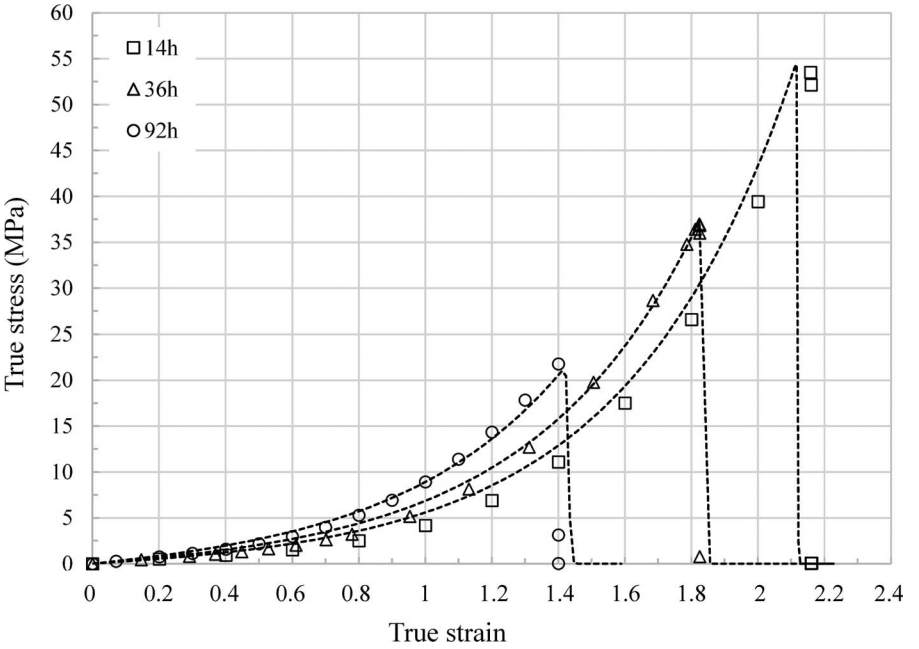


FIG. 11. — Modeling (dashed lines) of the stress–strain response in tension (symbols) of the industrial material after 14, 36, and 92 h of thermal aging in air at 170 °C.

The main advantage of the proposed model is that all its parameters are experimentally accessible, and most of them (in particular, rate constants) obey an Arrhenius law. This model can be used for analyzing, understanding, and interpreting experimental results of industrial materials operating under service conditions. It can be also used for predicting the lifetime if the relevant structural or mechanical end-of-life criterion is known.

REFERENCES

[1]N. Semenov, *Chemical Kinetics and Chain Reactions*, Clarendon Press, Oxford, UK, 1929.

[2]H. Staudinger and H. F. Bondy, RUBBER CHEM. TECHNOL. **3**, 519 (1930).

[3]J. L. Bolland and G. Gee, *Trans. Faraday Soc*. **42**, 236 (1946).

[4]J. L. Bolland and G. Gee, *Trans. Faraday Soc*. **42**, 244 (1946).

[5]A. V. Tobolsky, D. J. Metz, and R. B. Mesrobian, *J. Am. Chem. Soc*. **72**, 1942 (1950).

[6]J. L. Bolland, *Quart. Rev*. **3**, 1 (1949).

[7]E. M. Bevilacqua, *J. Am. Chem. Soc*. **77**, 5394 (1955).

[8]E. M. Bevilacqua, *J. Polym. Sci*. **49**, 495 (1961).

[9]F. R. Mayo, *Ind. Eng. Chem*. **52**, 614 (1960).

[10]A. Charlesby, *J. Polym. Sci*. **11**, 513 (1953).

[11]A. Charlesby, *Proc. R. Soc*. **222A**, 542 (1954).

[12]P. J. Flory, *Principles of Polymer Chemistry*, Cornell University Press, Ithaca, NY, 1953.

[13]L. M. Rincon-Rubio, X. Colin, L. Audouin, and J. Verdu, RUBBER CHEM. TECHNOL. **76**, 460 (2003).

[14]X. Colin, E. Richaud, J. Verdu, and C. Monchy-Leroy, *Radiat. Phys. Chem*. **79**, 365 (2010).

[15]M. Baba, J. Nedelec, J. Lacoste, J. Gardette, and M. Morel, *Polym. Degrad. Stability* **80**, 305 (2003).

[16]F. Grasland, "Ageing by Thermal Oxidation of Natural Rubber: Studies of its Consequences on Crystallization under Deformation, Cracking and Fracture," Ph.D. Thesis, INSA, Lyon, France, 2018.

[17]S. Howse, C. Porter, T. Mengistu, I. Petrov, and R. J. Pazur, RUBBER CHEM. TECHNOL. **92**, 513 (2019).

[18]P. Ghosh, S. Katare, P. Patkar, J. M. Caruthers, V. Venkatasubramanian, and K. A. Walker, RUBBER CHEM. TECHNOL. **76**, 592 (2003).

[19]O. H. Yeoh, RUBBER CHEM. TECHNOL. **85**, 482 (2012).

[20]L. Achimsky, L. Audouin, J. Verdu, J. Rychly, and L. Matisova-Rychla, *Polym. Degrad. Stability* **58**, 283 (1997).

[21]X. Colin, L. Audouin, and J. Verdu, *Polym. Degrad. Stability* **92**, 906 (2007).

[22]F. Delor-Jestin, "Long Term Thermal and Photochemical Behavior of Elastomers for Applications in the Automotive Field," Ph.D. Thesis, Blaise Pascal University, Clermont-Ferrand, France, 1996.

[23]M. Ben Hassine, "Modelling of the Thermal and Mechanical Ageing of an External EPDM Protection of Cold Shrinkable Junction," Ph.D. Thesis, ENSAM, Paris, 2013.

[24]M. Ben Hassine, M. Naït-Abdelaziz, F. Zaïri, X. Colin, C. Tourcher, and G. Marque, *Mech. Mater.* **79**, 15 (2014).

[25]Y. Kamiya and E. Niki, "Oxidative Degradation," in *Aspects of Degradation and Stabilization of Polymers*, H. H. G. Jellinek, Ed., Elsevier, New York, 1978, p. 86.

[26]S. Korcek, J. H. B. Chenier, J. A. Howard, and K. U. Ingold, *Can. J. Chem.* **50**, 2285 (1972).

[27]N. Khelidj, X. Colin, L. Audouin, J. Verdu, C. Monchy-Leroy, and V. Prunier, *Polym. Degrad. Stability* **91**, 1598 (2006).

[28]X. Colin, L. Audouin, and J. Verdu, RUBBER CHEM. TECHNOL. **80**, 621 (2007).

[29]A. François-Heude, E. Richaud, A. Guinault, E. Desnoux, and X. Colin, *J. Appl. Polym. Sci.* **132**, 41441 (2015).

[30]X. Colin, L. Audouin, and J. Verdu, *Polym. Degrad. Stability* **86**, 309 (2004).

[31]X. Colin, C. Marais, and J. Verdu, *J. Appl. Polym. Sci.* **82**, 3430 (2001).

[32]N. Khelidj, X. Colin, L. Audouin, J. Verdu, C. Monchy-Leroy, and V. Prunier, *Polym. Degrad. Stability* **91**, 1593 (2006).

[33]H. Zweifel, *Plastics Additives Handbook*, 5th ed., Hanser, Munich, 2001.

[34]P. Mulder, O. W. Saastad, and D. Griller, *J. Am. Chem. Soc.* **110**, 4090 (1988).

[35]F. G. Bordwell and X. M. A. N. Zhang, *J. Phys. Org. Chem.* **8**, 529 (1995).

[36]Q. Zhu, X.-M. Zhang, and A. J. Fry, *Polym. Degrad. Stability* **57**, 43 (1997).

[37]J. Pospisil, *Polym. Degrad. Stability* **40**, 217 (1993).

[38]J. Pospisil, *Polym. Degrad. Stability* **39**, 103 (1993).

[39]R. J. Shelton, "Stabilization against Thermal Oxidation," in *Polymer Stabilization*, W. L. Hawkins, ed., Wiley-Interscience, New York, 1971, p. 67.

[40]J. P. Roberts and K. U. Ingold, *J. Am. Chem. Soc.* **95**, 3228 (1973).

[41]A. Faucitano, A. Buttafava, F. Martinotti, and P. Bortulus, *J. Phys. Chem.* **88**, 1187 (1984).

[42]J. Sedlar, J. Petruj, J. Pac, and M. Navratil, *Polymer* **21**, 5 (1980).

[43]J. Sedlar, J. Petruj, J. Pac, and A. Zahradnickova, *Eur. Polym. J.* **16**, 663 (1980).

[44]T. D. W. Grattan, D. J. Carlsson, J. A. Howard, and D. M. Wiles, *Can. J. Chem.* **57**, 2834 (1979).

[45]T. A. B. M. Bolsman, A. P. Blok, and J. H. G. Frijns, *Recueil des Travaux Chimiques des Pays-Bas* **97**, 313 (1978).

[46]L. Bateman and J. Cunneen, RUBBER CHEM. TECHNOL. **29**, 3056 (1956).

[47]J. Colclough, J. L. Cunneen, and G. M .C. Higgins, *J. Appl. Polym. Sci.* **12**, 295 (1968).

[48]D. Barnard and P. M. Lewis, "Oxidative Aging," in *Natural Rubber Science and Technology*, A. D. Roberts, Ed., Oxford University Press, New York, 1988, p. 624.

[49]X. Colin, L. Audouin, M. Le Huy, and J. Verdu, *Polym. Degrad. Stability* **92**, 898 (2007).

[50]J. R. Shelton, RUBBER CHEM. TECHNOL. **30**, 1251 (1957).

[51]E. M. Bevilacqua, *Autooxidation and Antioxidants,* vol. 2, W. O. Lundberg, Ed., Interscience Publications, New York, 1962, Ch. 18.

[52]G. Milani, E. Leroy, F. Milani, and R. Deterre, *Polym. Test*. **32**, 1052 (2013).

[53]O. Saito, *J. Phys. Soc. (Japan)* **13**, 198 (1958).

[54]O. Saito, *J. Phys. Soc. (Japan)* **13**, 1451 (1958).

[55]H. M. James and E. Guth, *J. Chem. Phys*. **11**, 455 (1943).

[56]S. Wu, *J. Polym. Sci. Part B Polym. Phys*. **27**, 723 (1989).

[57]X. Colin, C. Monchy-Leroy, L. Audouin, and J. Verdu, *Nucl. Instrum. Methods Phys. Res*. **B265**, 251 (2007).

[58]X. Colin, L. Audouin, J. Verdu, M. Rozental-Evesque, B. Rabaud, F. Martin, and F. Bourgine, *Polym. Eng. Sci*. **49**, 1429 (2009).

[59]A. Mikdam, X. Colin, G. Minard, N. Billon, and R. Maurin, *Polym. Degrad. Stability* **146**, 78 (2017).

[60]M. Da Cruz, L. Van Schoors, K. Benzarti, and X. Colin, *J. Appl. Polym. Sci*. **133**, 43287 (2016).

[61]E. Hairer and G. Wanner, *Solving Ordinary Differential Equations II. Stiff and Differential-Algebraic Problems,* Springer, Berlin, 1991.

[*Presented at the Fall 194th Technical Meeting of the Rubber Division, ACS (Louisville, KY), 9–11 October 2018*]

[*Received November 2018, Revised April 2019*]

APPENDIX A: THERMAL OXIDATION KINETICS OF A STABILIZED AND SULFUR VULCANIZED EPDM

The general mechanistic scheme used for describing the thermal oxidation of a stabilized and sulfur vulcanized EPDM can be summarized as follows. It is composed of 17 reactions:

Initiation:

(1u) $\mathrm{POOH} \rightarrow 2\mathrm{P}^{\bullet} + \gamma_1\mathrm{P{=}O} + (1-\gamma_1)\mathrm{P-OH} + \mathrm{H_2O} + \upsilon\mathrm{V} + \gamma_S\mathrm{S}$ (k_{1u})

(1b) $2\mathrm{POOH} \rightarrow \mathrm{P}^{\bullet} + \mathrm{PO_2^{\bullet}} + \gamma_1\mathrm{P{=}O} + (1-\gamma_1)\mathrm{P-OH} + \mathrm{H_2O} + \upsilon\mathrm{V} + \gamma_S\mathrm{S}$ (k_{1b})

(1p) $\mathrm{POOP} \rightarrow 2\mathrm{P}^{\bullet} + 2\gamma_1\mathrm{P{=}O} + 2(1-\gamma_1)\mathrm{P-OH} + 2\upsilon\mathrm{V} - \mathrm{X} + 2\gamma_S\mathrm{S}$ (k_{1p})

Propagation:

(2) $\mathrm{P}^{\bullet} + \mathrm{O_2} \rightarrow \mathrm{PO_2^{\bullet}}$ (k_2)

(3) $\mathrm{PO_2^{\bullet}} + \mathrm{PH} \rightarrow \mathrm{POOH} + \mathrm{P}^{\bullet}$ (k_3)

Bimolecular combination:

(4) $\mathrm{P}^{\bullet} + \mathrm{P}^{\bullet} \rightarrow \gamma_4\mathrm{P-P} + (1-\gamma_4)\mathrm{PH} + (1-\gamma_4)\mathrm{F} + \gamma_4\mathrm{X}$ (k_4)

(5) $\mathrm{P}^{\bullet} + \mathrm{PO_2^{\bullet}} \rightarrow \gamma_5\mathrm{POOP} + (1-\gamma_5)\mathrm{POOH} + (1-\gamma_5)\mathrm{F} + \gamma_5\mathrm{X}$ (k_5)

(6a) $\mathrm{PO_2^{\bullet}} + \mathrm{PO_2^{\bullet}} \rightarrow [\mathrm{PO^{\bullet\bullet}OP}]_{\mathrm{cage}} + \mathrm{O_2}$ (k_{6a})

(6b) $[PO^{\bullet\bullet}OP]_{cage} \rightarrow POOP + X$ (k_{6b})

(6c) $[PO^{\bullet\bullet}OP]_{cage} \rightarrow P{=}O + P - OH$ (k_{6c})

(6d) $[PO^{\bullet\bullet}OP]_{cage} \rightarrow 2P^{\bullet} + 2\gamma_1 P{=}O + 2(1-\gamma_1)P - OH + 2\upsilon V + 2\gamma_S S$ (k_{6d})

Addition onto double bonds:

(7a) $P^{\bullet} + F_{ENB} \rightarrow P - P + P^{\bullet} + X$ (k_{7a})

(7b) $PO_2^{\bullet} + F_{ENB} \rightarrow POOP + P^{\bullet} + X$ (k_{7b})

Stabilization by molecular antioxidants:

(8) $AH + PO_2^{\bullet} \rightarrow B^{\bullet} + POOH$ (k_8)

(9) $B^{\bullet} + PO_2^{\bullet} \rightarrow$ inactive products (k_9)

(10) $O_2 + {>}NH \rightarrow {>}N^{\bullet}$ (k_{10})

(11) $PO_2^{\bullet} + {>}NH \rightarrow POOH + {>}N^{\bullet}$ (k_{11})

(12) ${>}N^{\bullet} + O_2 \rightarrow {>}NO_2^{\bullet}$ (k_{12})

(13) ${>}NO_2^{\bullet} + {>}NO_2^{\bullet} \rightarrow {>}NO^{\bullet} + {>}NO^{\bullet} + O_2$ (k_{13})

(14) ${>}NO^{\bullet} + P^{\bullet} \rightarrow {>}NOP$ (k_{14})

(15) $PO_2^{\bullet} + {>}NOP \rightarrow POOH + {>}NO^{\bullet} + F$ (k_{15})

Stabilization by sulfur bridges:

(16) $P_2S + POOH \rightarrow PSOR - \gamma_{16}C - S - \gamma_{16}X$ (k_{16})

(17) $PSO_iR + 4POOH \rightarrow PSO_{i+1}R - (1+\gamma_{17})C - S - (1+\gamma_{17})X$ (k_{17})

where

(a) PH accounts for the secondary hydrogen atom under consideration along the EPDM polymer chain
(b) $P^{\bullet}$, $PO_2^{\bullet}$, and $PO^{\bullet}$ account respectively for alkyl, peroxy, and alkoxy radicals
(c) POOH, POOP, P=O, and P–OH account respectively for hydroperoxides, dialkyl peroxides, carbonyls, and alcohols
(d) F_{ENB}, F, S and X account respectively for ethylidene and vinylene double bonds, chain scissions, and cross-linking nodes (i.e., covalent bridges)
(e) AH, >NH, $B^{\bullet}$, $>N^{\bullet}$, and $>NO^{\bullet}$ account respectively for hindered phenols, hindered amines, and their various active radicals
(f) P_2S, PSO_iR (with $i = 1, \ldots, 3$), and C–S account respectively for sulfide bridges, their oxidized sulfur structures, and carbon–sulfur bonds

(g) k_j and γ_j (with $j = 1, \ldots, 17$) are elementary rate constants and chemical yields, respectively

(h) From a practical point of view, it is more convenient to use an apparent yield γ_1 for the formation efficiency of carbonyls owing to the high uncertainty on the nature of these species, but also the value of their corresponding molar extinction coefficients[60]

(i) γ_S accounts for β-scission efficiency of $PO^\bullet$ radicals

(j) γ_4 and γ_5 account respectively for the coupling efficiency of radical species

(k) γ_{16} and γ_{17} account for the efficiency of the Colclough's mechanism,[47] which involves the breaking of a C–S bond

A system of 17 non-linear differential equations can be derived from this mechanistic scheme for reactive species only, by applying the classical rules of chemical kinetics

$$\frac{d[\mathrm{POOH}]}{dt} = -k_{1u}[\mathrm{POOH}] - 2k_{1b}[\mathrm{POOH}]^2 + k_3\left[PO_2^\bullet\right][\mathrm{PH}] + (1-\gamma_5)k_5[P^\bullet]\left[PO_2^\bullet\right] + k_8[\mathrm{AH}]\left[PO_2^\bullet\right] + k_{11}\left[PO_2^\bullet\right][>\mathrm{NH}] + k_{15}\left[PO_2^\bullet\right][>\mathrm{NOP}] - k_{16}[P_2S][\mathrm{POOH}] - 4k_{17}[\mathrm{POS_iR}][\mathrm{POOH}] \quad (A1)$$

$$\frac{d[P^\bullet]}{dt} = 2k_{1u}[\mathrm{POOH}] + k_{1b}[\mathrm{POOH}]^2 + 2k_{1p}[\mathrm{POOP}] - k_2[O_2][P^\bullet] + k_3\left[PO_2^\bullet\right][\mathrm{PH}] - 2k_4[P^\bullet]^2 - k_5[P^\bullet]\left[PO_2^\bullet\right] + 2k_{6d}[PO^{\bullet\bullet}OP]_{\mathrm{cage}} + k_{7b}\left[PO_2^\bullet\right][F_{\mathrm{ENB}}] - k_{14}[>NO^\bullet][P^\bullet] \quad (A2)$$

$$\frac{d\left[PO_2\right]}{dt} = k_{1b}[\mathrm{POOH}]^2 + k_2[O_2][P^\bullet] - k_3\left[PO_2^\bullet\right][\mathrm{PH}] - k_5[P^\bullet]\left[PO_2^\bullet\right] - 2k_{6a}\left[PO_2^\bullet\right]^2 - k_{7b}\left[PO_2^\bullet\right][F_{\mathrm{ENB}}] - k_8[\mathrm{AH}]\left[PO_2^\bullet\right] - k_9[B^\bullet]\left[PO_2^\bullet\right] - k_{11}\left[PO_2^\bullet\right][>\mathrm{NH}] - k_{15}\left[PO_2^\bullet\right][>\mathrm{NOP}] \quad (A3)$$

$$\frac{d[PO^{\bullet\bullet}OP]_{\mathrm{cage}}}{dt} = k_{6a}\left[PO_2^\bullet\right]^2 - (k_{6b} + k_{6c} + k_{6d})[PO^{\bullet\bullet}OP]_{\mathrm{cage}} \quad (A4)$$

$$\frac{d[\mathrm{PH}]}{dt} = -(2+\gamma_S)k_{1u}[\mathrm{POOH}] - (1+\gamma_S)k_{1b}[\mathrm{POOH}]^2 - 2(1+\gamma_S)k_{1p}[\mathrm{POOP}] - k_3\left[PO_2^\bullet\right][\mathrm{PH}] - (1-\gamma_5)k_5[P^\bullet]\left[PO_2^\bullet\right] - 2(1+\gamma_S)k_{6d}[PO^{\bullet\bullet}OP]_{\mathrm{cage}} - \gamma_{16}k_{16}[P_2S][\mathrm{POOH}] - (1+\gamma_{17})k_{17}[\mathrm{POS_iR}][\mathrm{POOH}] \quad (A5)$$

$$\frac{d[F_{\mathrm{ENB}}]}{dt} = -k_{7a}[P^\bullet][F_{\mathrm{ENB}}] - k_{7b}\left[PO_2^\bullet\right][F_{\mathrm{ENB}}] \quad (A6)$$

$$\frac{d[\mathrm{POOP}]}{dt} = -k_{1p}[\mathrm{POOP}] + \gamma_5 k_5[P^\bullet]\left[PO_2^\bullet\right] + k_{6b}[PO^{\bullet\bullet}OP]_{\mathrm{cage}} + k_{7b}\left[PO_2^\bullet\right][F_{\mathrm{ENB}}] \quad (A7)$$

$$\frac{d[\mathrm{AH}]}{dt} = -\mathrm{k}_8[\mathrm{AH}]\left[\mathrm{PO}_2^{\bullet}\right] \tag{A8}$$

$$\frac{d[\mathrm{B}^{\bullet}]}{dt} = \mathrm{k}_8[\mathrm{AH}]\left[\mathrm{PO}_2^{\bullet}\right] - \mathrm{k}_9[\mathrm{B}^{\bullet}]\left[\mathrm{PO}_2^{\bullet}\right] \tag{A9}$$

$$\frac{d[>\mathrm{NH}]}{dt} = -\mathrm{k}_{10}[\mathrm{O}_2][>\mathrm{NH}] - \mathrm{k}_{11}\left[\mathrm{PO}_2^{\bullet}\right][>\mathrm{NH}] \tag{A10}$$

$$\frac{d[>\mathrm{N}^{\bullet}]}{dt} = \mathrm{k}_{10}[\mathrm{O}_2][>\mathrm{NH}] + \mathrm{k}_{11}\left[\mathrm{PO}_2^{\bullet}\right][>\mathrm{NH}] - \mathrm{k}_{12}[>\mathrm{N}^{\bullet}][\mathrm{O}_2] \tag{A11}$$

$$\frac{d\left[>\mathrm{NO}_2^{\bullet}\right]}{dt} = \mathrm{k}_{12}[>\mathrm{N}^{\bullet}][\mathrm{O}_2] - 2\mathrm{k}_{13}\left[>\mathrm{NO}_2^{\bullet}\right]^2 \tag{A12}$$

$$\frac{d[>\mathrm{NO}^{\bullet}]}{dt} = 2\mathrm{k}_{13}\left[>\mathrm{NO}_2^{\bullet}\right]^2 - \mathrm{k}_{14}[>\mathrm{NO}^{\bullet}][\mathrm{P}^{\bullet}] + \mathrm{k}_{15}\left[\mathrm{PO}_2^{\bullet}\right][>\mathrm{NOP}] \tag{A13}$$

$$\frac{d[>\mathrm{NOP}]}{dt} = \mathrm{k}_{14}[>\mathrm{NO}^{\bullet}][\mathrm{P}^{\bullet}] - \mathrm{k}_{15}\left[\mathrm{PO}_2^{\bullet}\right][>\mathrm{NOP}] \tag{A14}$$

$$\frac{d[\mathrm{P_2S}]}{dt} = -\mathrm{k}_{16}[\mathrm{P_2S}][\mathrm{POOH}] \tag{A15}$$

$$\frac{d[\mathrm{PSO}_i\mathrm{R}]}{dt} = \mathrm{k}_{16}[\mathrm{P_2S}][\mathrm{POOH}] - \mathrm{k}_{17}[\mathrm{PSO}_i\mathrm{R}][\mathrm{POOH}] \tag{A16}$$

$$\frac{d[\mathrm{C-S}]}{dt} = -\gamma_{16}\mathrm{k}_{16}[\mathrm{P_2S}][\mathrm{POOH}] - (1+\gamma_{17})\mathrm{k}_{17}[\mathrm{PSO}_i\mathrm{R}][\mathrm{POOH}] \tag{A17}$$

The initial conditions (when $\mathrm{t} = 0$) are

$$[\mathrm{POOH}] = [\mathrm{POOH}]_0$$

$$[\mathrm{P}^{\bullet}] = \left[\mathrm{PO}_2^{\bullet}\right] = [\mathrm{PO}^{\bullet\bullet}\mathrm{OP}]_{\mathrm{cage}} = [\mathrm{POOP}] = 0$$

$$[\mathrm{PH}] = [\mathrm{PH}]_0$$

$$[\mathrm{F_{ENB}}] = [\mathrm{F_{ENB}}]_0$$

$$[\mathrm{AH}] = [\mathrm{AH}]_0$$

$$[>\mathrm{NH}] = [>\mathrm{NH}]_0$$

$$[\mathrm{B}^{\bullet}] = [>\mathrm{N}^{\bullet}] = \left[>\mathrm{NO}_2^{\bullet}\right] = [>\mathrm{NO}^{\bullet}] = [>\mathrm{NOP}] = 0$$

$$[\mathrm{P_2S}] = [\mathrm{P_2S}]_0$$

$$[PSO_iR] = 0$$

$$[C - S] = [C - S]_0$$

Let us recall that, in the case of sufficiently thin samples for which oxidation is homogenous throughout their thickness (no formation of oxidation profiles), oxygen concentration is equal to its equilibrium value at any time:

$$[O_2] = [O_2]_0$$

The numerical methods for solving such a system of differential equations have been already described in previous publications, for instance in Kamiya and Niki.[25] Very briefly, they are based on implicit or semi-implicit algorithms recommended for solving "stiff problems" of chemical kinetics. Indeed, these algorithms give a satisfactory approximate solution for a reasonable cost of calculation. The results reported in this study were obtained by applying the ODE23s solver of Matlab commercial software based on the semi-implicit Rosenbrock's algorithm.[61]

Equations (A1) to (A17) were integrated numerically for accessing the concentration changes over time of exposure of all the reactive chemical species.

APPENDIX B: MATURATION/REVERSION KINETICS OF A SULFUR VULCANIZED EPDM

The following simplified mechanistic scheme was chosen for describing the maturation/reversion of a sulfur vulcanized EPDM. It is composed of two reactions:

(18) Prec $\rightarrow \gamma_{18} X_S + (1 - \gamma_{18}) X_U$ (k_{18})

(19) X_U $\rightarrow$ non − cross − linking products (k_{19})

where

(a) Prec accounts for post-cross-linking precursor
(b) X_S and X_U account respectively for stable and unstable sulfide bridges
(c) γ_{18} is a "partition coefficient" between stable and unstable sulfide bridges

A system of three linear differential equations can be derived from this mechanistic scheme, by applying the classical rules of chemical kinetics:

$$\frac{d[\text{Prec}]}{dt} = -k_{18}[\text{Prec}] \tag{B1}$$

$$\frac{dX_S}{dt} = \gamma_{18} k_{18}[\text{Prec}] \tag{B2}$$

$$\frac{dX_U}{dt} = (1 - \gamma_{18}) k_{18}[\text{Prec}] - k_{19} X_U \tag{B3}$$

The initial conditions (when $t = 0$) are

$$[\text{Prec}] = [\text{Prec}]_0$$

$$X_S = X_{S0}$$

$$X_U = X_{U0}$$

The same numerical methods indicated in Appendix A were used for solving this system of differential equations. Equations (B1) to (B3) were integrated numerically with the ODE23s solver of Matlab commercial software for accessing the concentration changes over time of exposure of these three chemical species.

Appendix C:
Lists of the Most Used Symbols: Chemical quantities

Notation	Meaning
AH	Hindered phenol antioxidant
$B^{\bullet}$	Radical quinonic structure
C–H	Carbon–hydrogen bond
C–S	Carbon–sulfur bond
F	Double bond
F_{ENB}	Ethylidene double bond
>NH	Hindered amine antioxidant
$>N^{\bullet}$	Aminyl radical
$>NO^{\bullet}$	Nitroxy radical
>NOP	Alkoxy amine
O_2	Oxygen
P–P	Dialkyl bridge
PH	Polymer chain
$P^{\bullet}$	Alkyl radical
$PO^{\bullet}$	Alkoxy radical
$[PO^{\bullet}\ {}^{\bullet}OP]_{cage}$	Pair of caged alkoxy radicals
P=O	Carbonyl
P–OH	Hydroxyl
$PO_2^{\bullet}$	Peroxy radical
POOH	Hydroperoxide
POOP	Dialkyl peroxide
Prec	Post-cross-linking precursor
P_2S	Sulfide bridge
P_2SO	Sulfoxide
PSOH	Sulfenic acid
P_2SO_2	Sulfone
PSO_2H	Sulfinic acid
PSO_3H	Sulfonic acid
S	Chain scission
SO_4H_2	Sulfuric acid
V	“Average” molecule of volatile compounds
X	Cross-linking event and cross-link node
X_S	Stable sulfide bridge
X_U	Unstable sulfide bridge

Appendix D:
List of the Most Used Symbols: Parameters

Notation	Meaning
b	Concentration in dangling chains
ξ	Chemical yield
ξ'	Chemical yield
f	Functionality of cross-link nodes
γ	Chemical yield
k	Rate constant
λ	True extension ratio
m	Mass of the polymer sample
M_C	Average molar mass of the elastically active chains
M_n	Number average molecular mass
M_V	Average molar mass of volatile compounds
M_W	Weight average molecular mass
n	Concentration in cross-link nodes
ν	Concentration in elastically active chains
p	Probability of the radical attack
r	Rate
R	Universal constant of perfect gas
ρ	Polymer density
σ	True tensile stress
T	Temperature
υ	Formation yield of volatile compounds